Pressure and Temperature Effect on Cellulose Hydrolysis Kinetic in Pressurized Water

Danilo A. Cantero[a,b], Ángel Sánchez Tapia[a], M. Dolores Bermejo[a] and M. José Cocero[a]

[a] High Pressure Processes Group, Department of Chemical Engineering and Environmental Technology, University of Valladolid, Prado de la Magdalena s/n, 47011 Valladolid, SPAIN

[b] Department of Applied and Industrial Chemistry. Faculty of Exact, Physical and Natural Sciences, National University of Cordoba, Av. Velez Sarsfield 1611, 5000, Cordoba, ARGENTINA

* Corresponding author, TEL: +34-983423166, FAX: +34-983423013, e-mail:

Abstract

In this study, the effect of temperature and pressure on cellulose and glucose hydrolysis in a hydrothermal media is analyzed. To do so, hydrolysis experiments were carried out in a continuous pilot plant capable of operating up to 400ºC, 27 MPa and residence times between 0.004 s and 40 s. This is possible using an instantaneous heating system by supercritical water injection and cooling by sudden depressurization of the hot product stream. Cellulose hydrolysis produced oligosaccharides, cellobiose, glucose and fructose. In general, concentration profiles of each component were similar for the same temperature and different pressures. Nevertheless, glucose and fructose hydrolysis reaction were strongly affected by changing the pressure, which is density. By increasing temperature and pressure, the reaction of glucose isomerization to fructose was inhibited, and the production of 5-hydroxymethylfurfural (5-HMF) through by fructose dehydration was also inhibited. On the other hand, 5-HMF production was favored by high hydroxide anion concentrations. Thus, at a constant temperature, the production of 5-HMF was increased by rising density (increasing pressure). The production of glycolaldehyde (retro-aldol condensation of glucose) was increased by increasing pressure and temperature. The reaction rates of cellulose hydrolysis were fitted using the experimental data. Pressure seems to have no effect on the cellulose hydrolysis kinetic to simple sugars, and at subcritical temperatures the kinetics of glucose hydrolysis reactions did not show significant changes by increasing pressure. However, at 400ºC glucose isomerization and dehydration reactions were diminished by increasing pressure while glucose retro-aldol condensation were enhanced.

Keywords: Activation Volume, Biorefinery, Glycolaldehyde, Ionic Product, Selectivity, 5-HMF

Notation

A	Pre-exponential factor of Arrhenius equation
E_a	Activation energy of Arrhenius equation ($kJ \cdot mol^{-1}$)
k	Reaction constant rate of cellulose hydrolysis (s^{-1})
k_{fa}	Reaction constant rate of fructose to organics acids (s^{-1})
k_{fg}	Reaction constant rate of fructose to glyceraldehyde (s^{-1})
k_{fh}	Reaction constant rate of 5-HMF production (s^{-1})
k_{ga}	Reaction constant rate of glucose to 1,6 anhydroglucose (s^{-1})
k_{gf}	Reaction constant rate of glucose to fructose (s^{-1})
k_{gg}	Reaction constant rate of glucose to glycolaldehyde (s^{-1})
k_{glyp}	Reaction constant rate of glyceraldehyde to pyruvaldehyde (s^{-1})
k_h	Reaction constant rate of cellobiose hydrolysis (s^{-1})
k_p	Reaction constant rate of pyruvaldehyde degradation (s^{-1})
K_w	Ionic product of water
l	length (m)
$\dot{M}$	Mass flow ($kg \cdot h^{-1}$)
n_i	concentration of component 'i' ($mol \cdot L^{-1}$)
P	Pressure (MPa)
R	Gas constant ($kJ \cdot K^{-1} \cdot mol^{-1}$)
S	Cross area of the tubular reactor (m^2)

T	Temperature (K)
t	Time (s)
t_r	Residence time (s)
W	Mass of cellulose (g)
X	Conversion
ρ	Density ($kg \cdot m^{-3}$)
$\Delta v^{\neq}$	Activation Volume ($cm^3 \cdot mol^{-1}$)

1. Introduction

Vegetal biomass chemical transformations have been intensively studied in the last years looking for a renewable sources of chemicals and fuels [1]. Cellulose is generally the major compound of vegetal biomass representing the most abundant biopolymer in nature[2]. Cellulose depolymerization was studied following different methods in order to obtain valuable compounds like soluble sugars [3-6], lactic acid [7] or 5-hydroxymethylfurfural (5-HMF) [8, 9] among others.

Cellulose conversion into these kind of products is dependent of the reaction medium and the reactions conditions. The use of supercritical fluids as reaction medium is a promising alternative in the biomass upgrading due to the possibility of tuning medium properties by changing pressure and temperature. Supercritical water (SCW) is water at temperature and pressure above its critical point (Tc=374ºC and Pc=22.1 MPa). The properties of water can be highly varied by changing pressure and temperature in the neighborhood of its critical point. The different identities that water could take by changing pressure and temperature will affect the reaction medium favoring some kind of reactions over others. Two important properties of water as reaction medium are density and ionic product. The density of the medium is a measurement of the water molecules population per volume. The water concentration is an important factor to take into account in the reactions where water participates, both as reagent or forming intermediate states[10]. The ionic product of water (Kw) represents how dissociated are water molecules (ion concentration). This property could be modified in order to favor or disfavor the acid/basis catalysis. The variations of these two properties of water in the surroundings of the critical point are shown in figure 1 [11, 12]. Significant variations in density and ionic product can be obtained at 400ºC by increasing pressure in the range 150 – 300 bar. However, at subcritical temperatures changes in properties with pressure are softer than at 400ºC (less than 10%). Important changes in the identity of the medium can be obtained if temperature and pressure are changed at the same time. For example, density of water at 300ºC and 27 MPa is around 750 kg/m^3; this value can be decreased to 130 kg/m^3 if the conditions are modified to 400ºC and 23MPa. Ion product of water at 300ºC and 27 MPa is around 10^{-11} $mol^2.l^{-2}$ which means that medium has high concentration of ions ($[H^+]$ and

[OH^-]) favoring the ionic reactions [13-15]. The ionic product of water will take a value of 10^{-21} $mol^2.l^{-2}$ if the temperature and pressure are changed to 400ºC and 23 MPa favoring radical reactions [16].

Cellulose hydrolysis in pressurized water medium was studied in different kind of reactors; batch [17-19], semi-continuous [20] and continuous [3, 21-27]. Batch experiments of cellulose hydrolysis can be done with quite simple equipment allowing fast and non-expensive results. However, the process control (t_r, T) is poor, making difficult to obtain products with high selectivity. Therefore, the products of these kinds of processes are usually divided into fractions: bio-oils; water soluble; solids and; gases. The main difficulty of the continuous process is the steady supply of cellulose (solid, non-soluble in water) to the reactor due to the possible pump clogging However, this problem can be overcome by scaling-up of the process using higher flows [1]. The hydrolysis and modification of cellulose in a hydrothermal medium can be controlled in a continuous reactor by simply varying T, P and t_r. Hence, the continuous process allows higher selectivity than the batch processes. So far, the maximum selectivity achieved by continuous cellulose hydrolysis was almost 70% w/w and less than 20% w/w for soluble sugars or fragmented products respectively [21-23, 27]. Recently, our research group could improve the selectivity obtaining sugars or pyruvaldehyde selectivity of 98% w/w and 40% w/w respectively by using a novel reactor [3]. The sugars obtained after biomass hydrolysis were susceptible to be further modified in a hot pressurized water medium in order to obtain high added value products like glycolaldehyde, poly-alcohols or 5-hidroxy-methyl-furfural (5-HMF) [13, 28-30].

In this work, the effect of pressure and temperature (medium properties) on cellulose hydrolysis in a hydrothermal medium were analyzed and the experimental data were used to fit kinetics parameters of the reactions involved.

2. Materials and Methods

2.1. Materials

113 Microcrystalline cellulose (99%) used in the experiments was purchased from VWR. Distilled
114 water was used as reaction medium in the experiments. The standards used in HPLC (High
115 Performance Liquid Chromatography) analysis were: cellobiose (+98%), glucose (+99%),
116 fructose (+99%), glyceraldehyde (95%), pyruvaldehyde (40%), glycolaldehyde dimer (99%),
117 levulinic acid (+99%), (5-HMF) 5-hydroxymethylfurfural (99%) purchased from Sigma.

118 *2.2. Analysis*

119 The cellulose conversion was determined by equation 1, where X is the cellulose conversion, W_0
120 is the inlet cellulose concentration measured in g cellulose/g total, W is the outlet cellulose
121 concentration measured in g cellulose/g total.

122 $$X = \frac{W_0 - W}{W_0} \quad (1)$$

123 The carbon content of the liquid products was determined by total organic carbon (TOC) analysis
124 with Shimadzu TOC-VCSH equipment. The composition of the liquid products was determined
125 by High Performance Liquid Chromatography (HPLC) analysis. The HPLC column used for the
126 separation of the compounds was Sugar SH-1011 Shodex at 50ºC using H_2SO_4 (0.01 N) as mobile
127 phase with a flow rate of 0.8mL/min. A Waters IR detector 2414 was used to identify and quantify
128 the sugars and their derivatives. An UV-Vis detector was used to determine the 5-hidroxy-methyl-
129 furfural (5-HMF) concentration at a wavelength of 254nm.

130 *2.3. Experimental set-up*

131 A continuous pilot plant designed to operate at 400ºC was used to perform the experiments. A
132 scheme of the experimental set up is presented in figure 2. The cellulose hydrolysis pilot plant
133 could operate at temperatures up to 400ºC and pressures of up to 30 MPa. A cellulose suspension
134 (7% w/w) was continuously pumped up to the operation pressure and remains at room temperature
135 until the inlet of the reactor. In that point it is instantaneously heated by mixing it with a
136 supercritical water stream. In this way, heating of cellulose (start of the reactions) is achieved
137 almost instantaneously [3]. Mixing ratio of cold and hot streams mixing was chosen in order to
138 obtain a biomass concentration at the reactor inlet of approximately 1.5% w/w. Reactor effluent

was cooled (stopping the reaction) by sudden expansion obtaining an instantaneous cooling from the reaction temperature to 100 ± 10ºC. More detailed descriptions of the pilot plant and the operation procedure were presented in a previous work[3].

The main achievements of the experimental setup are: (a) the reactor can be considered isothermal due to the instantaneous heating and cooling; (b), products are not diluted in the cooling process; (c) the residence time is varied from 0.004 s to 40 s using Ni-alloy tubular reactors of different lengths.

3. Reaction Modeling

The reaction pathway of cellulose hydrolysis can be analyzed by dividing it in three main steps: 1) cellulose hydrolysis to produce oligosaccharides; 2) hydrolysis of oligosaccharides to produce glucose and; 3) the different glucose degradation reactions (isomerization, dehydration or retro-aldol condensation). A schema (figure 3) of the supposed reaction pathway was built from reaction pathways found in literature [31, 32]. A detailed analysis of the two first steps of cellulose hydrolysis was presented in a previous work [33]. In this work, the kinetics analysis was focused in glucose hydrolysis reactions. In figure 3 it is shown that glucose could follow two main degradation pathways: isomerization step to form fructose and then dehydration or retro aldol condensation to produce glycolaldehyde and erythrose; erythrose also follows a retro-aldol condensation producing glycolaldehyde as final product. So, one glucose molecule produces three molecules of glycolaldehyde.

A mathematical model was built in order to calculate concentrations profiles of the main derivatives of cellulose hydrolysis along the residence time at different conditions of pressure and temperature. The model was developed taking into account the OH^- concentration in the reactions of glucose isomerization and fructose dehydration. The role of hydroxyl anion concentration was analyzed in a previous work PAPER ANGE. The concentration of glucose was calculated as shown in equation 2. Where n_g is the concentration of glucose in $mol \cdot L^{-1}$ (M); z is the length of the reactor in m; ρ is the density of the reaction medium in $kg \cdot m^{-3}$; S is the cross section of the

tubular reactor in m^2 and; *M* is the mass flow through the reactor in $kg \cdot s^{-1}$. The kinetic parameters used in equation 2 were obtained in a previous work [33]. The molar concentration of each component was represented as *n* (mol/L), where the subscripts: *og, cello and OH* refer to oligosaccharides, cellobiose and hydroxyls respectively. CW_{og} is the carbon weight of the oligosaccharide monomer molecule (g/mol). MW_{og} is the molecular weight of the oligosaccharide monomer molecule. The constants were represented as *k* (s^{-1}), where the subscripts: *og*, *h*, *gf*, *gg* and *ga* refer to oligosaccharide hydrolysis, cellobiose hydrolysis, glucose to fructose isomerization, glucose to glycolaldehyde and, glucose dehydration.

$$\frac{dn_g}{dz} = \frac{\rho S}{\dot{M}}\left[k_{og} n_{og} \frac{CW_{og}}{CW_g MW_g} + 2k_h n_{cello} - \left(k_{gf} n_{OH} + k_{gg} + k_{ga}\right) n_g\right] \quad (2)$$

The concentration of fructose was determined as shown in equation 3, where n_f is the molar concentration of fructose (M). The subscripts *fh*, *fa* and *fg* refer to 5-HMF formation, fructose to acids and fructose retro aldol condensation reactions. The units of the reaction rates for k_{gf} and k_{fh} were $L \cdot mol^{-1} \cdot s^{-1}$.

$$\frac{dn_f}{dl} = \frac{\rho S}{\dot{M}}\left[k_{gf} n_g n_{OH} - \left(k_{fh} n_{OH} + k_{fa} + k_{fg}\right) n_f\right] \quad (3)$$

The concentration of 5-HMF was calculated as shown in equation 4, where n_h is the molar concentration of 5-HMF (M).

$$\frac{dn_h}{dl} = \frac{\rho S}{\dot{M}}\left[k_{fh} n_{OH} n_f\right] \quad (4)$$

The concentrations of glycolaldehyde and glyceraldehyde were calculated by equation 5 and 6 respectively.

$$\frac{dn_{glyco}}{dl} = \frac{\rho S}{\dot{M}}\left[3k_{gg} n_g\right] \quad (5)$$

$$\frac{dn_{gly}}{dl} = \frac{\rho S}{\dot{M}}\left[2k_{fg}n_f - k_{glyp}n_{gly}\right] \quad (6)$$

Where n_{glyco} is the molar concentration of glycolaldehyde; n_{gly} is the molar concentration of glyceraldehyde and; k_{glyp} is the kinetic constant of the reaction of glyceraldehyde to pyruvaldehyde isomerization. Pyruvaldehyde concentration was calculated in the same way than Cantero et al [33] by equation 7.

$$\frac{dn_{pyr}}{dl} = \frac{\rho S}{\dot{M}}\left[k_{glyp}n_{gly} - k_p n_p\right] \quad (7)$$

The values of the kinetics constants k_{og}, k_{gf}, k_{fh}, k_{gg} and k_{fg} were fitted by comparing the experimental concentration profiles to the profiles calculated by the model using the Matlab® function *lsqcurvefit*. Further information about model resolution can be found in a previous work [33].

4. Results and discussion

The reactions of cellulose hydrolysis in hot pressurized water were analyzed at 300ºC (10 MPa, 18 MPa, 23 MPa and 27 MPa), 350ºC (10 MPa, 18 MPa and 23 MPa) and 400ºC (23 MPa, 25 MPa and 27 MPa). In this range of conditions, the density (ρ) of the medium was varied from 150 to 750 $kg \cdot m^{-3}$; the ionic product (pKw) was varied from 11 to 21 $mol^2 \cdot kg^2$ and the dielectric constant (ε) was varied from 2 to 22. The carbon balance between the inlet and outlet of the reactor were in the range 88 – 100% for all the experiments.

4.1. Experimental concentration profiles

4.1.1. Cellulose hydrolysis kinetics

The results of cellulose conversion along residence time at 400ºC, 350ºC and 300ºC are shown in figure 4-A, 4-B and 4-C respectively. The lowest residence times tested for 400ºC were 15 ms, 13 ms and 17 ms for 23 MPa, 25 MPa and 27 MPa respectively. At those residence times no cellulose was found in the products and thus, the conversion was X=1 for all the experimental

conditions analyzed at 400ºC. In a previous work, the residence time for total cellulose conversion at 25 MPa was determined to be 15 ms [3]. At 350ºC and 300ºC pressure seems to have no effect in the kinetics of cellulose depolymerization. Experimental data shown in figure 4 were used to obtain the kinetics of cellulose hydrolysis according equation 8. Where X is the cellulose conversion (determined experimentally by equation 1); t is the residence time (s) and; k is the kinetic constant of cellulose hydrolysis (s^{-1}) as proposed by Sasaki et al [31].

$$\frac{dX}{dt} = 2k(1-X)^{1/2} \quad (8)$$

The k values were plotted in figure 5 along with the analogous values developed for a pressure of 25 MPa [33]. Similar values were obtained, showing that the pressure had no effect on the kinetics of cellulose hydrolysis in the studied range of pressure. If the kinetics of cellulose hydrolysis is analyzed along temperature, a break point around the critical point of water can be appreciated. At temperatures higher than 374ºC the depolymerization reaction rate is increased faster than at lower temperatures. This phenomenon can be explained considering that cellulose could be dissolved in supercritical water due to the change of the reaction medium identity. Therefore, the reaction of hydrolysis would occur in a homogeneous phase, avoiding the mass transfer limitations [31, 33].

4.1.2.Cellobiose

The concentration profiles of cellobiose (glucose disaccharide) at different pressures along residence time at 400ºC, 350ºC and 300ºC are shown in figure 6-A, 6-B and 6-C respectively. The peak concentration of cellobiose was achieved at each temperature were at residence times of 0.016 s, 2 s and 15 s for 400ºC, 350ºC and 300ºC respectively, being highest concentration at the maximum temperature 400ºC and the lowest pressure (23MPa). Thus, the cellobiose production was reduced when the pressure was increased and reaction temperature was reduced. These results agree with those found in literature [21], if it is had into account that, the maximum cellobiose selectivity is obtained at lower temperatures if the lowest analyzed residence time is higher than 1 second [27].

234 *4.1.3.Glucose*

235 The glucose concentration profiles along residence time at different pressures at 400ºC, 350ºC
236 and 300ºC were plotted in figure 6-D, 6-E and 6-F respectively. The glucose production followed
237 a similar behavior than that of cellobiose. Nevertheless, high quantities of glucose were found in
238 all the experimented temperatures. The literature data show high glucose selectivity (14 – 35 %
239 w/w) at 300ºC [22, 23, 26, 27]. The disadvantage of working at 350ºC or 300ºC is that high
240 residence times are needed which also favor the reactions of glucose hydrolysis, and favoring the
241 apparition of other compounds.

242 *4.1.4.Fructose*

243 The fructose concentrations along residence time at different pressures at 400ºC, 350ºC and 300ºC
244 are shown in figure 6-G, 6-H and 6-I respectively. The highest selectivity of fructose were
245 achieved at 400ºC and 350ºC at a residence time around 0.3 s and 2 s respectively. The maximum
246 concentrations of fructose were lower than the concentration of cellobiose and glucose (almost
247 20% compared with glucose). Although the peak concentration of fructose at 400ºC was found at
248 25 MPa and 27 MPa (one experimental point), for the other analyzed residence times the higher
249 concentrations were achieved at a pressure of 23 MPa. The reaction of glucose isomerization to
250 produce fructose takes place via ring-opening producing several transition states (keto-enol
251 tautomerism). This reaction was slowed down when pressure was increased. Kabyemela et al [34]
252 obtained a similar behavior working in glucose hydrolysis. They concluded that the reaction of
253 glucose isomerization to produce fructose is retarded by increasing pressure when the working
254 temperature is above the critical point of water.

255 *4.1.5. Glyceraldehyde*

256 The glyceraldehyde concentration along residence time at the experimented pressures and
257 temperatures are shown in figure 7-A, 7-B and 7-C. The maximum amount of glyceraldehyde was
258 achieved at 400ºC and 350ºC with residence times of 0.5 s and 2 s respectively. In this case, the
259 pressure seems to have no effect in the production of glyceraldehyde at 350ºC or 300ºC. However,
260 at 400ºC the concentration of glyceraldehyde was slightly increased by decreasing the pressure.

261 *4.1.6. Glycolaldehyde*

262 The values of glycolaldehyde concentration obtained at different pressures for 400ºC, 350ºC and
263 300ºC are shown in figure 7-D, 7-E and 7-F respectively. The maximum concentration of
264 glycolaldehyde (around 8000 ppm) was achieved at 400ºC, 27 MPa and 1 s of residence time. An
265 increase in the pressure improved the production of glycolaldehyde for all the experimented
266 temperatures. If the concentration profiles of glycolaldehyde are analyzed along temperature, it
267 is observed that increasing temperature, the production of glycolaldehyde was highly increased
268 in the studied range. Peak concentrations of glycolaldehyde at 300 and 350ºC were around 3000
269 ppm and 4000 respectively.

270 *4.1.7.5-HMF*

271 The 5-HMF concentration profiles obtained at 400ºC, 350ºC and 300ºC were plotted in figure 7-
272 G, 7-H and 7-I respectively. The production of 5-HMF was highly inhibited at temperatures
273 higher than the critical temperature of water. The maximum concentration was obtained at the
274 lowest experimented temperature with 25 s of residence time. For all the experimented
275 temperatures, an increase in pressure increased the production of 5-HMF. Different data about the
276 5-HMF behavior can be found in literature. Ehara et al [2222] and Sasaki et al [21] obtained low
277 concentration of 5-HMF at supercritical conditions (≈0.1% w/w). Nevertheless, Zhao et al [23]
278 and Kumar et al [27] obtained similar values of 5-HMF selectivity at sub and supercritical
279 conditions (≈8% w/w).

280 *4.2. Kinetics Model*

281 The reaction rates of glucose to fructose isomerization (k_{gf}), fructose to 5-HMF dehydration (k_{fh}),
282 glucose to glycolaldehyde retro aldol condensation (k_{gg}) and fructose retro-aldol condensation
283 (k_{fg}) were fitted for all the experimental conditions using the concentration data profiles along
284 residence time according the method explained in section 3. The activation energy (E_a) and pre-
285 exponential factor ($Ln\ k_0$) for each kinetic was determined at 23 MPa and 27 MPa according
286 equation 9 (Arrhenius relationship). Where k is the reaction rate (s^{-1}); R is the gas constant (kJ K^{-}

287 ^{1} mol^{-1}) and; T is the temperature (K). The Arrhenius parameters are shown in table 1 and are
288 analyzed in sections 4.2.1. to 4.2.5.

289 $$\ln k = \ln k_0 - \frac{E_a}{R}\frac{1}{T} \quad (9)$$

290 The influence of pressure in the reaction kinetics can be analyzed by using the concept of
291 activation volume ($\Delta v^{\neq}$) that is defined as the excess of the partial molar volume of the transition
292 state over the partial molar volume of the initial species [35]. The relationship between the
293 kinetics dependence with pressure and the activation volume is shown in equation 10. Where $\Delta v^{\neq}$
294 is the activation volume in cm^3·mol^{-1}; P is pressure in bar and; R is the gas constant (83.14
295 cm^3·bar·mol^{-1}·K^{-1}).

296 $$\left.\frac{\partial \ln k}{\partial P}\right|_T = -\frac{\Delta v^{\neq}}{RT} \quad (10)$$

297 Sometimes the activation volume can be divided into two terms as it is shown in equation 11 [36].
298 Where $\Delta v_1^{\neq}$ represents the molar volume difference between the transition state and the reactants
299 and; $\Delta v_2^{\neq}$ represents the interactions between the reactants and solvent molecules. If a reactive
300 system shows more attractive potential between solvent and transition state, than between solvent
301 and reactant; the reaction rate would be enhanced by rising pressure [37].

302 $$\Delta v^{\neq} = \Delta v_1^{\neq} + \Delta v_2^{\neq} \quad (11)$$

303 The second term is usually the most important when the reactions occurs in conditions near the
304 critical point of the solvent. Although the typical values of $\Delta v^{\neq}$ ranges between -60 and 30 cm^3
305 mol^{-1}; in the surroundings of the critical point the volume of activation can reach values greater
306 than ±1000 cm^3·mol^{-1} [38] because the phenomenon is amplified due to near divergence of the
307 isothermal compressibility of the medium [37]. The fitted values of $\Delta v^{\neq}$ for k_{gf}, k_{fh}, k_{gg} and k_{fg} are
308 listed in table 2 and are analyzed in sections 4.2.2. to 4.2.5.

309

310 *4.2.1.Glucose isomerization to fructose (k_{gf})*

311 The kinetic constants of glucose isomerization to produce fructose at different temperatures and
312 pressures are shown in Figure 8. At 300ºC and 350ºC the pressure showed to have almost no
313 effect in the reaction rate. However, when the temperature was increased until 400ºC, the kinetic
314 constants were reduced when pressure was increased. It is observed that by increasing the reaction
315 temperature, the pressure has a negative effect in the reaction rate. At 23 MPa the E_a and Ln k_0
316 were 516 ± 182 kJ·mol^{-1} and 117 ± 35 respectively (see Table 1). The activation volume of k_{gf}
317 took a value of 3226 ± 194 cm^3·mol^{-1} at 400ºC (see Table 2). However, at subcritical temperatures
318 the activation volume was small, being the pressure effect negligible. The activation volume was
319 high and positive at 400ºC, meaning that the reaction of glucose isomerization is inhibited when
320 pressure is increased. This phenomenon would mean that the interaction between the transition
321 state of glucose-fructose (ring opening and keto-enol tautomerism by hydroxyl/proton transfer
322 [39]) and the solvent is less attractive than the interaction of glucose with supercritical water
323 (solvent).

324 *4.2.2. Fructose dehydration to 5-HMF (k_{fh})*

325 The fitted kinetic constants at the studied temperatures and pressures were plotted in Figure 9.
326 The activation energy and pre-exponential factor were slightly decreased (≈3%) by increasing
327 pressure from 23 MPa to 27MPa (see Table 1). The E_a and Ln k_0 for k_{fh} took values of 463.7 ±
328 160.6 kJ·mol^{-1} and 104.6 ± 31.2 respectively at 23 MPa. The kinetic constant is decreased by
329 rising pressure at 400ºC. However, the values of activation volume for 300ºC and 350ºC showed
330 little variations. The fitted values of $\Delta v^{\neq}$ are listed in Table 2.

331 *4.2.3. Glucose to glycolaldehyde reaction (k_{gg})*

332 The reaction rates of glycolaldehyde production from glucose at different temperature are plotted
333 against pressure in Figure 10. Contrary than the kinetic constant of glucose isomerization, k_{gg} was
334 increased at 400ºC when pressure was increased. At 300ºC and 350ºC, pressure showed to have
335 almost no effect in the kinetic of glucose to glycolaldehyde reaction. The values of E_a and Ln k_0

for the kinetic of glycolaldehyde production from glucose at 23 and 27 MPa are shown in Table 1. The activation energy and pre-exponential factor were almost the same when pressure was increased from 23 MPa to 27 MPa. The volumes of activation at 350ºC and 400ºC are shown in Table 2. The activation volume was -201 ± 5 $cm^3 \cdot mol^{-1}$ at 400ºC. In this case the volumes of activation were negatives. Following with the discussion of section 4.2.2., the activation volume value of k_{gg} would mean that the interaction of the transition state of glucose-glyceraldehyde with the solvent is more attractive than the interaction between glucose and supercritical water (solvent). Accordingly, it can be concluded that at 400ºC when pressure is increased from 23 MPa to 27 MPa, the reaction of glycolaldehyde production is improved while the reaction of glucose epimerization to give fructose is diminished.

4.2.4. Fructose retro aldol condensation (k_{fg})

Glyceraldehyde production kinetic constants are plotted against pressure at different temperature in Figure 11. The pressure effect in this reaction was negligible at subcritical temperatures. The values of activation energy for this reaction rate at 23 MPa and 27 MPa were 115.3 ± 2.6 $kJ \cdot mol^{-1}$ and 180.6 ± 36.0 $kJ \cdot mol^{-1}$ respectively. The pre-exponential factors were 22.8 ± 0.5 and 35.8 ± 7.0 for 23 MPa and 27 MPa respectively. The activation volumes at subcritical temperatures were near to zero (k_{fg} do not change appreciable with pressure) and that is why the error of the linear fit was high. If the activation value of k_{fg} at 400ºC is analyzed join whit k_{fh}, it can be seen that k_{fg} is improved by increasing pressure while k_{fh} is decreased.

4.2.5. Global parameters

For reactors design, it would be interesting to get an equation that relates the kinetic of the reactions with temperature and pressure at the same time. For this purpose equation 12 was proposed.

$$k = k_0 e^{\frac{-E_a}{RT}} e^{\frac{-\Delta v^{\neq} P}{RT}} \quad (12)$$

The global activation energy, pre-exponential factor (k_0) and the activation volume were fitted for each reaction kinetic using the fitting tool *sftool* of Matlab®. The fitted parameters are shown in Table 3. The adjusted parameters for the kinetics of k_{gf} and k_{fh} were fitted using the kinetics constants at 300ºC and 350ºC. The kinetic values at 400ºC were too high in comparison with the subcritical ones as it can be seen in Figures 8 and 9. So, it was not possible to fit values of *Ea*, *ko* and $\Delta v^{\neq}$ that represent the behavior of the kinetic in the whole range of temperature. Using the parameters shown in Table 3 for k_{gg} and k_{fg}*;* it is possible to calculate the kinetics contants over the entire analyzed range of pressure (10 – 27 MPa) and temperature (300 – 400ºC). In Figure 12 it is shown the calculated kinetic surface and the kinetics of the experimented points for the kinetic *kgg*.

5. Conclusions

Cellulose hydrolysis was studied experimentally in order to analyze the effect of pressure and temperature in the kinetics of cellulose and glucose in a hydrothermal medium. The experiments were carried out in the pressure range of 10 MPa – 27 MPa, at 300ºC, 350ºC and 400ºC. A mathematical model was built in order to fit the main reaction rates of glucose hydrolysis (k_{og}, k_{gf}, k_{gg}, k_{fh}, *and* k_{fg}).

The reactions of glucose hydrolysis were found to be highly influenced by temperature. Nevertheless, in general, pressure has a slight effect on the kinetics at subcritical temperatures, while at temperatures higher than the critical temperature of water, that influence can be remarkable: i.e. at 400ºC, the kinetic constant of glucose isomerization to fructose (k_{gf}) would be decreased when pressure is increased. At the contrary, the reaction of glucose retro-aldol condensation (k_{gg}) would be enhanced by raising pressure. The reaction of 5-HMF production (k_{fh}) and oligosaccharides hydrolysis (k_{og}) would be enhanced by decreasing pressure. The cellulose hydrolysis reaction rate was not affected by pressure in the studied range.

The Arrhenius parameters of the main glucose reactions in a hydrothermal medium were calculated at 23 and 27 MPa. Also, the activation volume was calculated at 300ºC, 350ºC and

386 400ºC. It was observed that the activation volume was small at subcritical temperatures,
387 nevertheless, at supercritical temperatures the activation volume was high.

388 **Acknowledgements**

389 The authors thank the Spanish Ministry of Science and 513 Innovation for the Project CTQ2011-
390 23293 and ENE2012-33613. The authors thank Repsol for its technical support. D.A.C. thanks
391 the Spanish Ministry of Education for the FPU fellowship (AP2009-0402).

392 References
393
394 [1] A.A. Peterson, F. Vogel, R.P. Lachance, M. Fröling, Michael J. Antal, Jr., J.W. Tester,
395 Thermochemical biofuel production in hydrothermal media: A review of sub- and supercritical
396 water technologies, Energy & Environmental Science, 1 (2008) 32-65.
397 [2] D. Klemm, B. Heublein, H.P. Fink, A. Bohn, Cellulose: Fascinating Biopolymer and
398 Sustainable Raw Material, Angewandte Chemie International Edition, 44 (2005) 3358-3393.
399 [3] D.A. Cantero, M.D. Bermejo, M.J. Cocero, High glucose selectivity in pressurized water
400 hydrolysis of cellulose using ultra-fast reactors, Bioresource Technology, 135 (2013) 697-703.
401 [4] Y. Zhao, H.-T. Wang, W.-J. Lu, H. Wang, Combined supercritical and subcritical conversion
402 of cellulose for fermentable hexose production in a flow reaction system, Chemical Engineering
403 Journal, 166 (2011) 868-872.
404 [5] P. Lenihan, A. Orozco, E. O'Neill, M.N.M. Ahmad, D.W. Rooney, G.M. Walker, Dilute acid
405 hydrolysis of lignocellulosic biomass, Chemical Engineering Journal, 156 (2010) 395-403.
406 [6] Y. Xiong, Z. Zhang, X. Wang, B. Liu, J. Lin, Hydrolysis of cellulose in ionic liquids catalyzed
407 by a magnetically-recoverable solid acid catalyst, Chemical Engineering Journal, 235 (2014) 349-
408 355.
409 [7] C. Sánchez, I. Egüés, A. García, R. Llano-Ponte, J. Labidi, Lactic acid production by alkaline
410 hydrothermal treatment of corn cobs, Chemical Engineering Journal, 181–182 (2012) 655-660.
411 [8] B. Liu, Z. Zhang, Z.K. Zhao, Microwave-assisted catalytic conversion of cellulose into 5-
412 hydroxymethylfurfural in ionic liquids, Chemical Engineering Journal, 215–216 (2013) 517-521.
413 [9] X. Qi, M. Watanabe, T.M. Aida, R.L.S. Jr, Catalytic conversion of cellulose into 5-
414 hydroxymethylfurfural in high yields via a two-step process, Cellulose, 18 (2011) 1327-1333.
415 [10] M. Akizuki, T. Fujii, R. Hayashi, Y. Oshima, Effects of water on reactions for waste
416 treatment, organic synthesis, and bio-refinery in sub- and supercritical water, Journal of
417 Bioscience and Bioengineering.
418 [11] W.L. Marshall, E.U. Franck, Ion Product of Water Substance, 0-1000ºC, 1-10,000 Bars. New
419 International Formulation and Its Backgroud, Journal of Physical and Chemical Reference Data,
420 10 (1981) 295-304.

421 [12] Wagner, W, Cooper, R. J, Dittmann, A, Kijima, J, Kretzschmar, J. H, Kruse, Mares, R,
422 Oguchi, K, Sato, H, St, Cker, I, Sifner, O, Takaishi, Y, Tanishita, Tr, Benbach, Willkommen, G.
423 T, The IAPWS industrial formulation 1997 for the thermodynamic properties of water and steam,
424 in, American Society of Mechanical Engineers, New York, N, ETATS-UNIS, 2000.
425 [13] T.M. Aida, Y. Sato, M. Watanabe, K. Tajima, T. Nonaka, H. Hattori, K. Arai, Dehydration
426 of D-glucose in high temperature water at pressures up to 80 MPa, The Journal of Supercritical
427 Fluids, 40 (2007) 381-388.
428 [14] N. Akiya, P.E. Savage, Roles of Water for Chemical Reactions in High-Temperature Water,
429 Chemical Reviews, 102 (2002) 2725-2750.
430 [15] A. Kruse, A. Gawlik, Biomass Conversion in Water at 330−410 °C and 30−50 MPa.
431 Identification of Key Compounds for Indicating Different Chemical Reaction Pathways,
432 Industrial & Engineering Chemistry Research, 42 (2002) 267-279.
433 [16] C. Promdej, Y. Matsumura, Temperature Effect on Hydrothermal Decomposition of Glucose
434 in Sub- And Supercritical Water, Industrial & Engineering Chemistry Research, 50 (2011) 8492-
435 8497.
436 [17] S. Yin, Z. Tan, Hydrothermal liquefaction of cellulose to bio-oil under acidic, neutral and
437 alkaline conditions, Applied Energy, 92 (2012) 234-239.
438 [18] K. Sakanishi, N. Ikeyama, T. Sakaki, M. Shibata, T. Miki, Comparison of the Hydrothermal
439 Decomposition Reactivities of Chitin and Cellulose, Industrial & Engineering Chemistry
440 Research, 38 (1999) 2177-2181.
441 [19] T. Minowa, F. Zhen, T. Ogi, Cellulose decomposition in hot-compressed water with alkali
442 or nickel catalyst, The Journal of Supercritical Fluids, 13 (1998) 253-259.
443 [20] T. Sakaki, M. Shibata, T. Sumi, S. Yasuda, Saccharification of Cellulose Using a Hot-
444 Compressed Water-Flow Reactor, Industrial & Engineering Chemistry Research, 41 (2002) 661-
445 665.
446 [21] M. Sasaki, Z. Fang, Y. Fukushima, T. Adschiri, K. Arai, Dissolution and Hydrolysis of
447 Cellulose in Subcritical and Supercritical Water, Industrial & Engineering Chemistry Research,
448 39 (2000) 2883-2890.

449 [22] K. Ehara, S. Saka, Decomposition behavior of cellulose in supercritical water, subcritical
450 water, and their combined treatments, Journal of Wood Science, 51 (2005) 148-153.
451 [23] Y. Zhao, W.-J. Lu, H.-T. Wang, Supercritical hydrolysis of cellulose for oligosaccharide
452 production in combined technology, Chemical Engineering Journal, 150 (2009) 411-417.
453 [24] Z. Fang, F. Zhang, H.-Y. Zeng, F. Guo, Production of glucose by hydrolysis of cellulose at
454 423 K in the presence of activated hydrotalcite nanoparticles, Bioresource Technology, 102
455 (2011) 8017-8021.
456 [25] A. Onda, T. Ochi, K. Yanagisawa, Hydrolysis of Cellulose Selectively into Glucose Over
457 Sulfonated Activated-Carbon Catalyst Under Hydrothermal Conditions, Topics in Catalysis, 52
458 (2009) 801-807.
459 [26] G. Brunner, Near critical and supercritical water. Part I. Hydrolytic and hydrothermal
460 processes, The Journal of Supercritical Fluids, 47 (2009) 373-381.
461 [27] S. Kumar, R.B. Gupta, Hydrolysis of Microcrystalline Cellulose in Subcritical and
462 Supercritical Water in a Continuous Flow Reactor, Industrial & Engineering Chemistry Research,
463 47 (2008) 9321-9329.
464 [28] T.M. Aida, K. Tajima, M. Watanabe, Y. Saito, K. Kuroda, T. Nonaka, H. Hattori, R.L. Smith
465 Jr, K. Arai, Reactions of D-fructose in water at temperatures up to 400 °C and pressures up to
466 100 MPa, The Journal of Supercritical Fluids, 42 (2007) 110-119.
467 [29] B.M. Kabyemela, T. Adschiri, R.M. Malaluan, K. Arai, Glucose and Fructose
468 Decomposition in Subcritical and Supercritical Water: Detailed Reaction Pathway, Mechanisms,
469 and Kinetics, Industrial & Engineering Chemistry Research, 38 (1999) 2888-2895.
470 [30] B.M. Kabyemela, T. Adschiri, R.M. Malaluan, K. Arai, H. Ohzeki, Rapid and Selective
471 Conversion of Glucose to Erythrose in Supercritical Water, Industrial & Engineering Chemical
472 Research, 36 (1997) 5063-5067.
473 [31] M. Sasaki, T. Adschiri, K. Arai, Kinetics of cellulose conversion at 25 MPa in sub- and
474 supercritical water, AIChE Journal, 50 (2004) 192-202.

[32] M. Sasaki, K. Goto, K. Tajima, T. Adschiri, K. Arai, Rapid and selective retro-aldol condensation of glucose to glycolaldehyde in supercritical water, Green Chem., 4 (2002) 285-287.

[33] D.A. Cantero, M.D. Bermejo, M.J. Cocero, Kinetic analysis of cellulose depolymerization reactions in near critical water, The Journal of Supercritical Fluids, 75 (2013) 48-57.

[34] B.M. Kabyemela, T. Adschiri, R. Malaluan, K. Arai, Degradation Kinetics of Dihydroxyacetone and Glyceraldehyde in Subcritical and Supercritical Water, Industrial & Engineering Chemistry Research, 36 (1997) 2025-2030.

[35] G. Luft, F. Recasens, E. Velo, Chapter 3 Kinetic properties at high pressure, in: A. Bertucco, G. Vetter (Eds.) Industrial Chemistry Library, Elsevier, 2001, pp. 65-140.

[36] D. Bröll, C. Kaul, A. Krämer, P. Krammer, T. Richter, M. Jung, H. Vogel, P. Zehner, Chemistry in Supercritical Water, Angewandte Chemie International Edition, 38 (1999) 2998–3014.

[37] S.F. Rice, R.R. Steeper, J.D. Aiken, Water Density Effects on Homogeneous Water-Gas Shift Reaction Kinetics, The Journal of Physical Chemistry A, 102 (1998) 2673-2678.

[38] P.E. Savage, S. Gopalan, T.I. Mizan, C.J. Martino, E.E. Brock, Reactions at supercritical conditions: Applications and fundamentals, AIChE Journal, 41 (1995) 1723–1778.

[39] Y. Román-Leshkov, M. Moliner, J.A. Labinger, M.E. Davis, Mechanism of Glucose Isomerization Using a Solid Lewis Acid Catalyst in Water, Angewandte Chemie International Edition, 49 (2010) 8954–8957.

Tables

Table 1

	P=23 MPa			P=27MPa		
	Ea kJ/mol	Ln Ao	R^2	Ea kJ/mol	Ln Ao	R^2
kgf	516 ± 182	117 ± 35	0.88	403 ± 97	94 ± 18	0.95
kfh	463 ± 160	104 ± 31	0.89	449 ± 95	101 ± 18	0.96
kgg	150.7 ± 26	28.0 ± 5.0	0.97	151.4 ± 32.7	28.4 ± 6.4	0.96
kfg	115.3 ± 2.6	22.8 ± 0.5	0.99	180.6 ± 36.0	35.8 ± 7.0	0.96

500 Table 2

	400°C		350°C		300°C	
	Δv^0 [cm^3/mol]	R^2	Δv^0 [cm^3/mol]	R^2	Δv^0 [cm^3/mol]	R^2
kgf	3226 ± 194	1.00	-82 ± 3	1.00	232 ± 34	0.96
kfh	1385 ± 171	0.98	-578 ± 160	0.93	363 ± 57	0.95
kgg	-201 ± 5	1.00	-229 ± 37	0.97	-28 ± 21	0.48
kfg	-1403 ± 329	0.95	-14 ± 122	0.01	68 ± 49	0.50

501

502 Table 3

	P=23 MPa			
	Ea kJ·mol^{-1}	Ln ko	∆V cm3·mol^{-1}	R^2
kgf	87.8	30.8	-158.4	0.91
kfh	105.8	27.7	-1011	0.85
kgg	106.7	-353.8	18.4	1.00
kfg	184.4	-2802.0	23.3	0.96

503

504 Figures

505 Figure 1

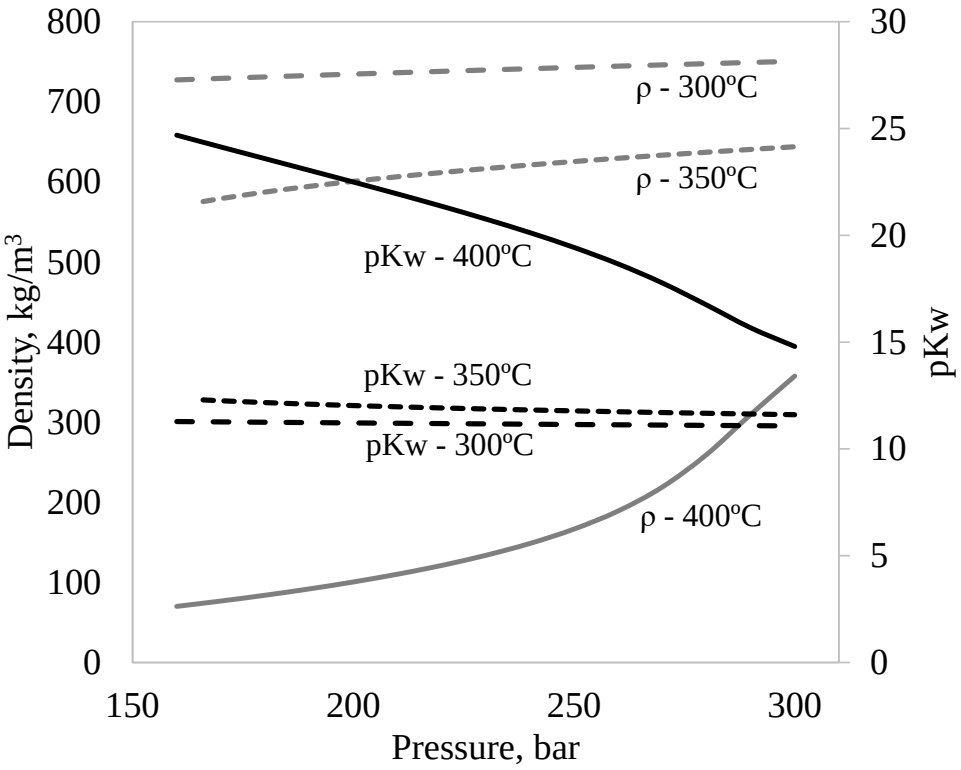

506

507 Figure 2

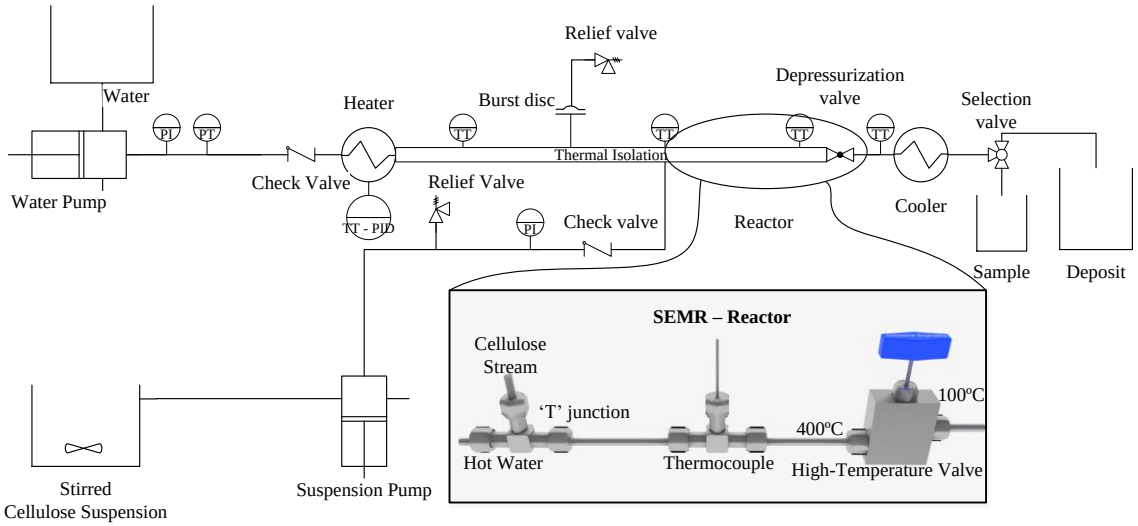

508

509 Figure 3

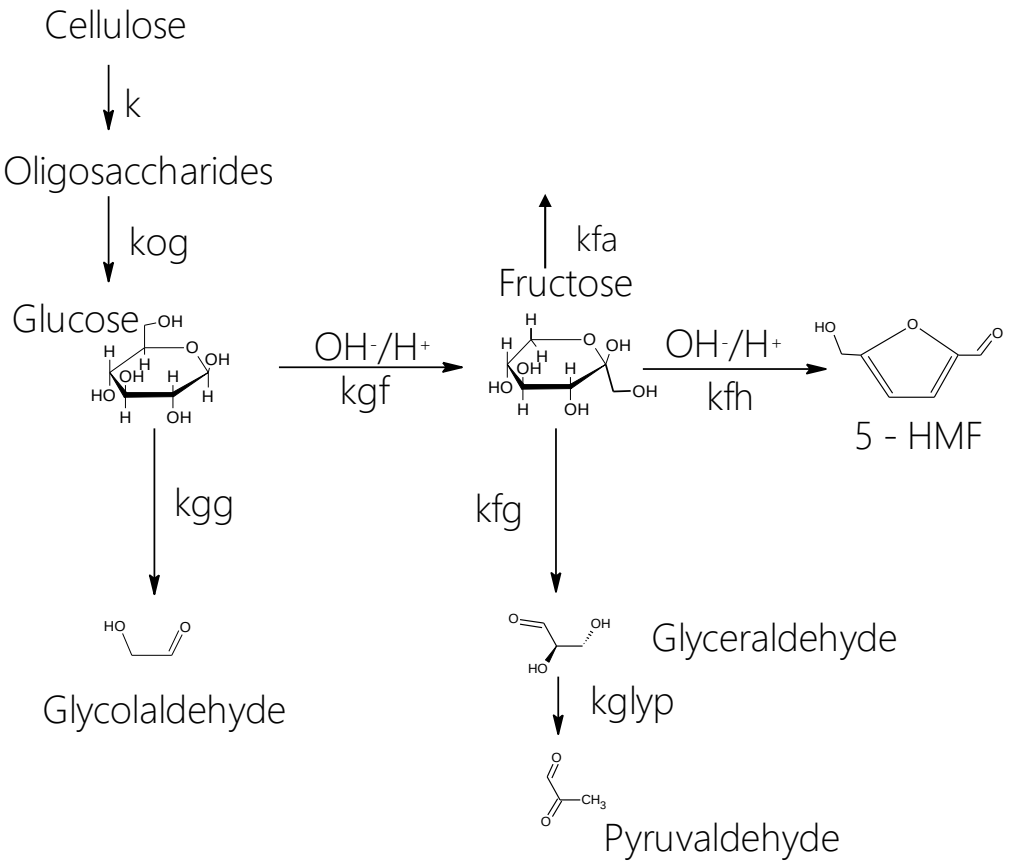

510

511 Figure 4

512 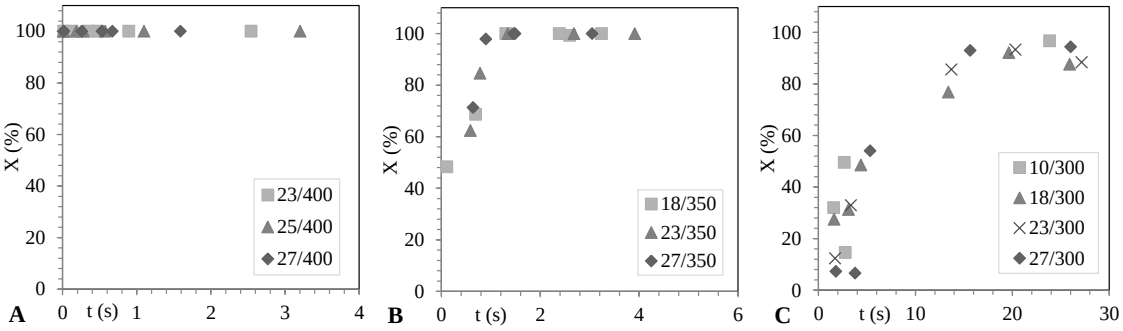

513 Figure 5

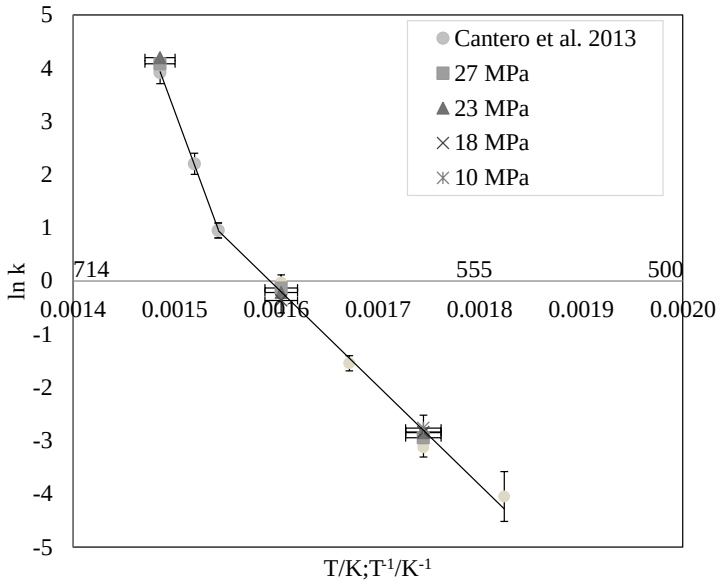

514

515 Figure 6

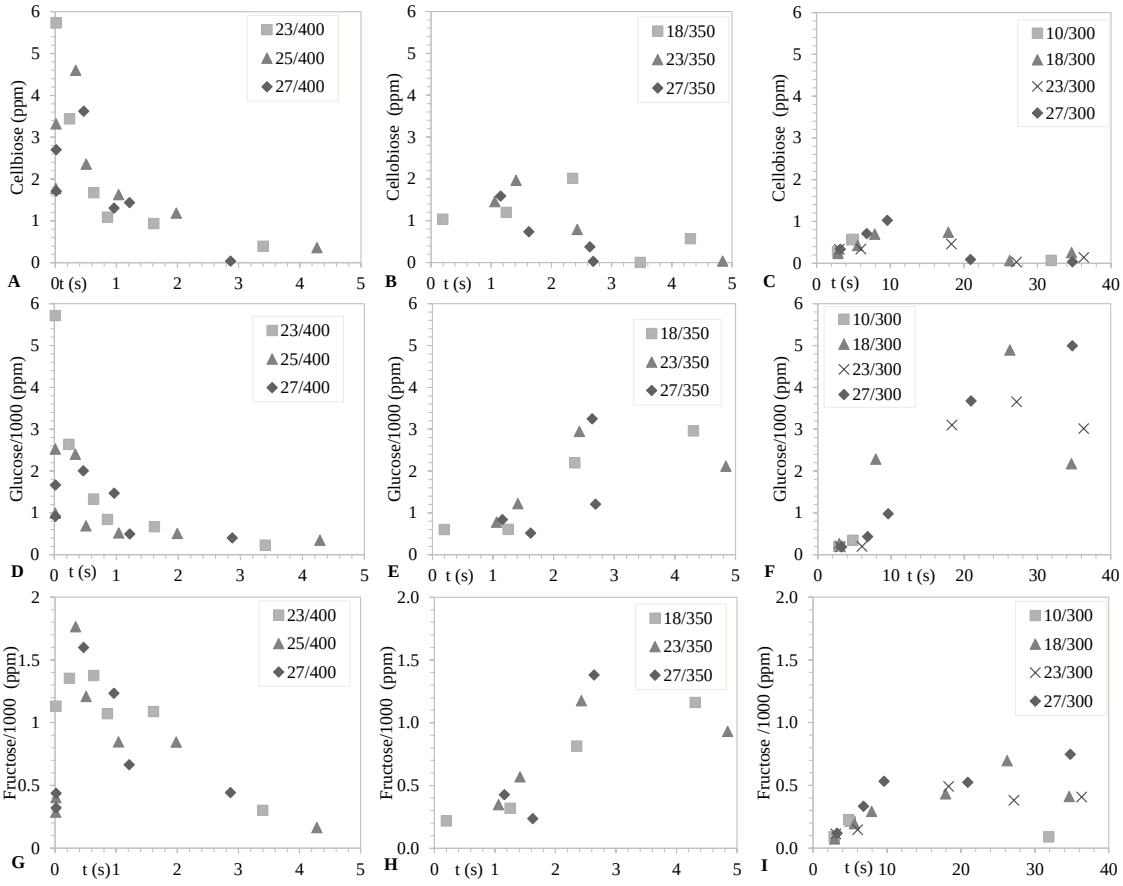

516

517 Figure 7

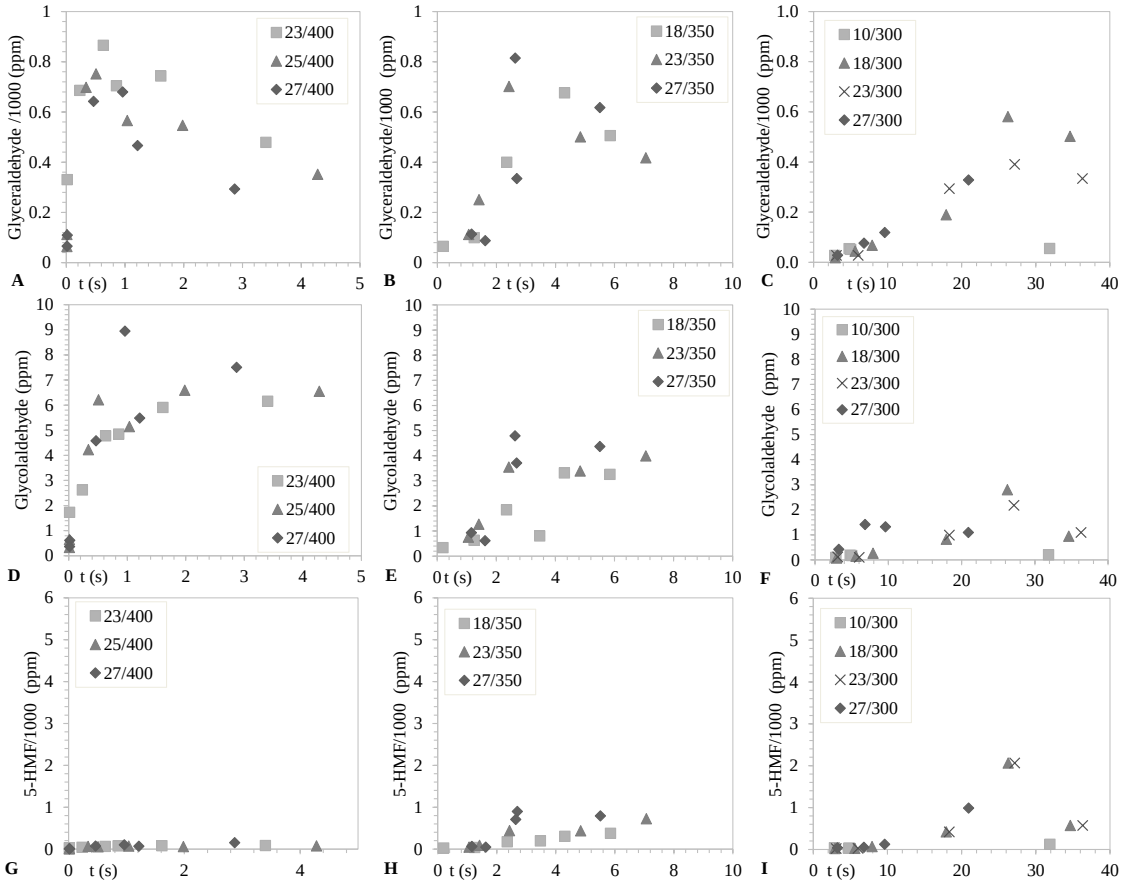

518

519 Figure 8

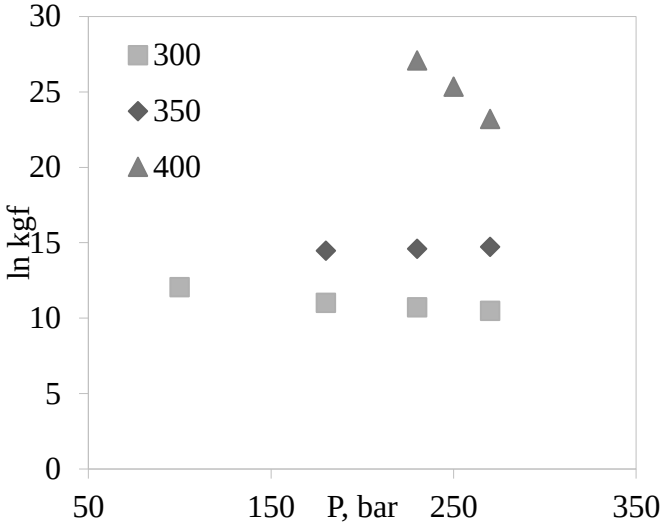

520

521 Figure 9

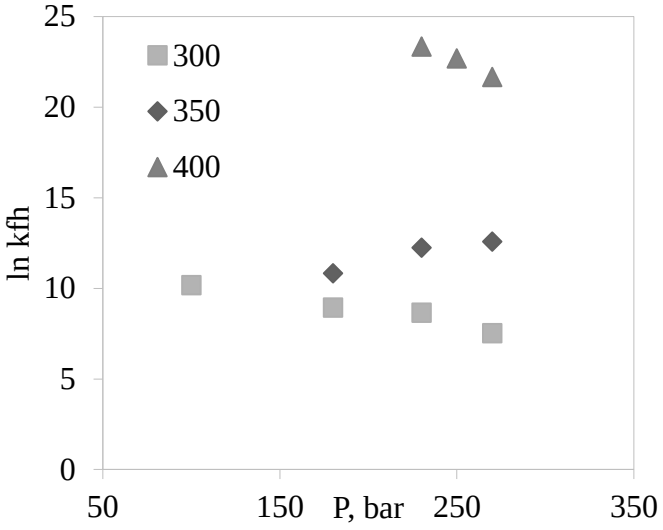

522

523 Figure 10

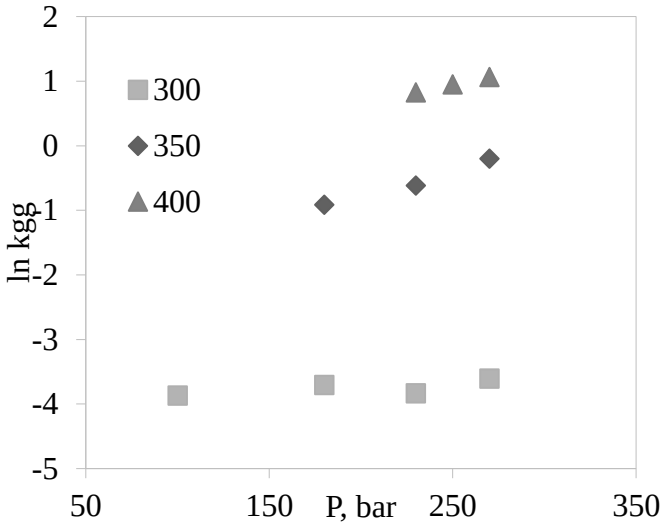

524

525 Figure 11

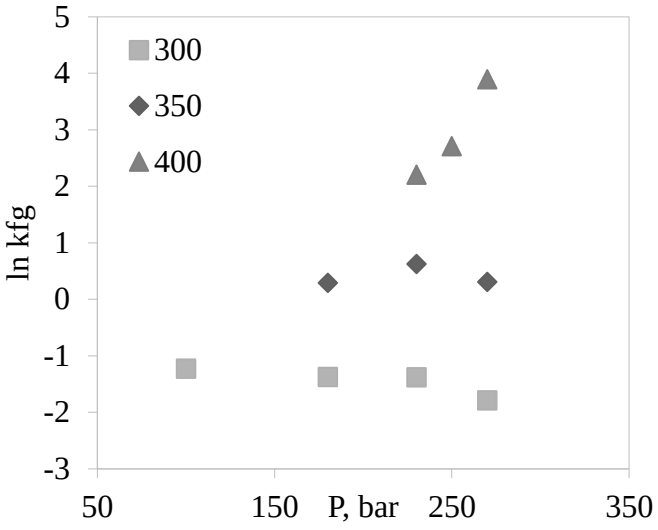

526

527

528 Figure 12

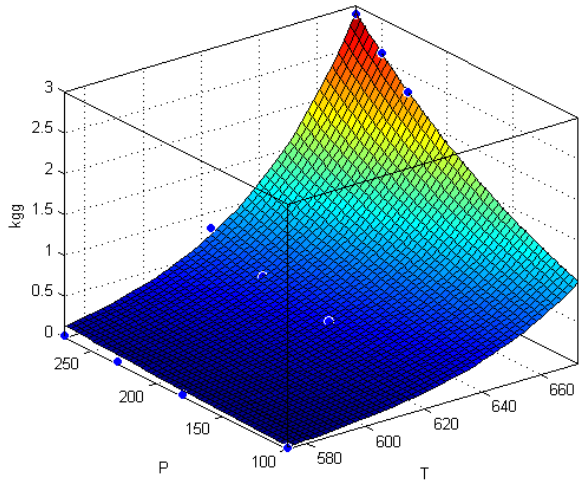

529

530 Table and Figure Captions

531 Table 1. Fitted Arrhenius parameters for the reactions of glucose in pressurized water.

532 Table 2. Fitted volumes of activation for the reactions of glucose in pressurized water.

533 Table 3. Global pre-exponential factors, activation energies and volumes of activation fitted for
534 the reactions of glucose in pressurized water.

535

536 Figure 1. Density and ionic product of water at different temperatures along pressure. Black lines:
537 minus logarithmic of ionic product; grey lines: density. Continuous lines refer to 400ºC; dashed
538 lines refer to 350ºC and spaced dashed lines refer to 300ºC.

539 Figure 2. Schema of the pilot plant.

540 Figure 3. Reaction pathway for cellulose and glucose hydrolysis in pressurized water.

541 Figure 4. (A) Cellulose conversion at 400ºC; (■) P= 23 MPa; (▲) P=25 MPa and; (♦) P= 27 MPa.
542 (B) Cellulose conversion at 350ºC; (■) P= 18 MPa; (▲) P=23 MPa and; (♦) P= 27 MPa. (C)
543 Cellulose conversion at 300ºC; (■) P= 10 MPa; (▲) P=18 MPa; (x) P=23 MPa and; (♦) P= 27
544 MPa.

545 Figure 5. Cellulose hydrolysis kinetics constant between 275ºC and 400ºC at (■) P= 27 MPa; (●)
546 P=25 MPa; (▲) P=23 MPa and; (x) P= 18 MPa and; (*) 10 MPa. The continuous line was taken
547 from an previous work [33]. Error bars (± s.d.).

548 Figure 6. (A) Cellobiose concentration at 400ºC; (■) P= 23 MPa; (▲) P=25 MPa and; (♦) P= 27
549 MPa. (B) Cellobiose concentration at 350ºC; (■) P= 18 MPa; (▲) P=23 MPa and; (♦) P= 27 MPa.
550 (C) Cellobiose concentration at 300ºC; (■) P= 10 MPa; (▲) P=18 MPa; (x) P=23 MPa and; (♦)
551 P= 27 MPa. (D) Glucose concentration at 400ºC; (■) P= 23 MPa; (▲) P=25 MPa and; (♦) P= 27
552 MPa. (E) Glucose concentration at 350ºC; (■) P= 18 MPa; (▲) P=23 MPa and; (♦) P= 27 MPa.
553 (F) Glucose concentration at 300ºC; (■) P= 10 MPa; (▲) P=18 MPa; (x) P=23 MPa and; (♦) P=

554 27 MPa. (G) Fructose concentration at 400ºC; (■) P= 23 MPa; (▲) P=25 MPa and; (♦) P= 27
555 MPa. (H) Fructose concentration at 350ºC; (■) P= 18 MPa; (▲) P=23 MPa and; (♦) P= 27 MPa.
556 (I) Fructose concentration at 300ºC; (■) P= 10 MPa; (▲) P=18 MPa; (x) P=23 MPa and; (♦) P=
557 27 MPa.

558 Figure 7. (A) Glyceraldehyde concentration at 400ºC; (■) P= 23 MPa; (▲) P=25 MPa and; (♦)
559 P= 27 MPa. (B) Glyceraldehyde concentration at 350ºC; (■) P= 18 MPa; (▲) P=23 MPa and; (♦)
560 P= 27 MPa. (C) Glyceraldehyde concentration at 300ºC; (■) P= 10 MPa; (▲) P=18 MPa; (x)
561 P=23 MPa and; (♦) P= 27 MPa. (D) Glycolaldehyde concentration at 400ºC; (■) P= 23 MPa; (▲)
562 P=25 MPa and; (♦) P= 27 MPa. (E) Glycolaldehyde concentration at 350ºC; (■) P= 18 MPa; (▲)
563 P=23 MPa and; (♦) P= 27 MPa. (F) Glycolaldehyde concentration at 300ºC; (■) P= 10 MPa; (▲)
564 P=18 MPa; (x) P=23 MPa and; (♦) P= 27 MPa. (G) 5-HMF concentration at 400ºC; (■) P= 23
565 MPa; (▲) P=25 MPa and; (♦) P= 27 MPa. (H) 5-HMF concentration at 350ºC; (■) P= 18 MPa;
566 (▲) P=23 MPa and; (♦) P= 27 MPa. (I) 5-HMF concentration at 300ºC; (■) P= 10 MPa; (▲)
567 P=18 MPa; (x) P=23 MPa and; (♦) P= 27 MPa.

568 Figure 8. Kinetic constant of glucose isomerization to fructose along pressure; (■) T= 300ºC; (♦)
569 T= 350ºC and; (▲) T=400ºC. (k_{gf}).

570 Figure 9. Kinetic constant of 5-HMF formation along pressure; (■) T= 300ºC; (♦) T= 350ºC and;
571 (▲) T=400ºC. (k_{fh}).

572 Figure 10. Kinetic constant of glucose retro-aldol condensation along pressure; (■) T= 300ºC; (♦)
573 T= 350ºC and; (▲) T=400ºC. (k_{gg}).

574 Figure 11. Kinetic constant of fructose retro-aldol condensation along pressure; (■) T= 300ºC; (♦)
575 T= 350ºC and; (▲) T=400ºC. (k_{fg}).

576 Figure 12. Kinetic constant (s^{-1}) of glucose retro-aldol condensation (k_{gg}) along pressure (bar) and
577 temperature (K).